Phys Chem Minerals (2001) 28: 413–420

ORIGINAL PAPER

H. Kojitani · A. Navrotsky · M. Akaogi

Calorimetric study of perovskite solid solutions in the $CaSiO_3$–$CaGeO_3$ system

Received: 20 September 2000 / Accepted: 17 January 2001

Abstract Enthalpies of drop solution ($\Delta H_{\text{drop-sol}}$) of $CaGeO_3$, $Ca(Si_{0.1}Ge_{0.9})O_3$, $Ca(Si_{0.2}Ge_{0.8})O_3$, $Ca(Si_{0.3}Ge_{0.7})O_3$ perovskite solid solutions and $CaSiO_3$ wollastonite were measured by high-temperature calorimetry using molten $2PbO \cdot B_2O_3$ solvent at 974 K. The obtained values were extrapolated linearly to the $CaSiO_3$ end member to give $\Delta H_{\text{drop-sol}}$ of $CaSiO_3$ perovskite of 0.2 ± 4.4 kJ mol^{-1}. The difference in $\Delta H_{\text{drop-sol}}$ between $CaSiO_3$, wollastonite, and perovskite gives a transformation enthalpy (wo $\rightarrow$ pv) of 104.4 ± 4.4 kJ mol^{-1}. The formation enthalpy of $CaSiO_3$ perovskite was determined as 14.8 ± 4.4 kJ mol^{-1} from lime + quartz or -22.2 ± 4.5 kJ mol^{-1} from lime + stishovite. A comparison of lattice energies among $A^{2+}B^{4+}O_3$ perovskites suggests that amorphization during decompression may be due to the destabilizing effect on $CaSiO_3$ perovskite from a large nonelectrostatic energy (repulsion energy) at atmospheric pressure. By using the formation enthalpy for $CaSiO_3$ perovskite, phase boundaries between β-Ca_2SiO_4 + $CaSi_2O_5$ and $CaSiO_3$ perovskite were calculated thermodynamically utilizing two different reference points [where $\Delta G(P,T) = 0$] as the measured phase boundary. The calculations suggest that the phase equilibrium boundary occurs between 11.5 and 12.5 GPa around 1500 K. Its slope is still not well constrained.

Key words Perovskite · $CaSiO_3$ · $CaGeO_3$ · Calorimetry · High-pressure phase transition

H. Kojitani · A. Navrotsky (✉)
Thermochemistry Facility,
Department of Chemical Engineering and Materials Science,
University of California at Davis, Davis,
CA 95616, USA
Tel.: +1 530 752 3292; Fax: +1 530 752-9307
e-mail: anavrotsky@ucdavis.edu

M. Akaogi
Department of Chemistry, Gakushuin University,
Mejiro, Toshima-ku, Tokyo 171-8588, Japan

Introduction

Recent high-pressure and high-temperature experiments indicate that $CaSiO_3$ perovskite is an important mineral constituent in the Earth's lower mantle. Irifune and Ringwood (1987) suggest that $CaSiO_3$ perovskite is the third most abundant phase after $(Mg,Fe)SiO_3$ perovskite and (Mg,Fe)O magnesiowüstite for a pyrolitic mantle composition under lower mantle conditions. Thus, the importance of understanding the behavior of $CaSiO_3$ perovskite at high pressure and high temperature is clear. In particular, quantification of the thermodynamic properties of $CaSiO_3$ perovskite is needed to assess its stability. However, $CaSiO_3$ perovskite amorphizes during pressure release (Liu and Ringwood 1975). This unquenchable character makes direct calorimetric measurements of $CaSiO_3$ perovskite under ambient pressure impossible. The instability has resulted in a lack of basic thermochemical data [e.g. formation enthalpy (ΔH_f°), entropy (S°), heat capacity (C_p°)] for pure $CaSiO_3$ perovskite. Instead, thermochemical data have been estimated using theoretical calculations and results of high-pressure and high-temperature experiments (e.g., Swamy and Dubrovinsky 1997). Recently, Koito et al. (2000) measured differential drop-solution enthalpies ($\Delta H_{\text{drop-sol}}$) at 1078 K of perovskite solid solutions in the $CaSiO_3$–$CaTiO_3$ system containing up to 50 mol% $CaSiO_3$ component. These data were used to estimate the enthalpy of the transition of $CaSiO_3$ wollastonite to perovskite. However, as Leinenweber et al. (1997) reported, $Ca(Ti_{0.5}Si_{0.5})O_3$ has an ordered double perovskite structure instead of the orthorhombic structure found for compositions with less than 50% $CaSiO_3$. The derived ΔH_f° of $CaSiO_3$ perovskite in the $CaSiO_3$–$CaTiO_3$ system, therefore, contains the uncertainty caused by this phase transition. To obtain a better constrained ΔH_f° of $CaSiO_3$ perovskite, further calorimetric data on $CaSiO_3$ perovskite-bearing systems are required.

Since the chemical behavior of Ge is similar to that of Si, a germanate material is often used as an analogue of a silicate mineral. $CaGeO_3$ also assumes a perovskite structure at about 6.5 GPa at 1273 K (Ross et al. 1986). $CaGeO_3$ perovskite is quenchable to ambient pressure. If quenchable perovskite solid solutions in the $CaSiO_3$–$CaGeO_3$ system are considered, their calorimetry will provide thermochemical information on $CaSiO_3$. Ringwood and Major (1967) reported that solid solubility of $CaSiO_3$ perovskite in $CaGeO_3$ perovskite was about 30 mol%. Hence, the $CaSiO_3$–$CaGeO_3$ system is another good candidate for obtaining ΔH_f° of $CaSiO_3$ perovskite by calorimetry.

In this study, we synthesized perovskite solid solutions in the $CaSiO_3$–$CaGeO_3$ system under high pressure and high temperature and performed calorimetry on the samples by using an "ultrasensitive" calorimeter, which is an improved Calvet-type twin microcalorimeter (Topor and Navrotsky 1992). From the estimated $\Delta H_{\text{drop-sol}}$ of $CaSiO_3$ perovskite, a new ΔH_f° for $CaSiO_3$ perovskite based on calorimetric data is presented. Our ΔH_f° for $CaSiO_3$ perovskite is compared to values reported by Koito et al. (2000) and by Swamy and Dubrovinsky (1997). In addition, we discuss the crystal chemistry of $A^{2+}B^{4+}O_3$ perovskites by applying the lattice energy approach used by Takayama-Muromachi and Navrotsky (1988). Finally, the ΔH_f° for $CaSiO_3$ perovskite obtained in this study is applied to the thermodynamic calculation of the high-pressure and high-temperature phase equilibrium boundaries in the $CaSiO_3$ system between β-Ca_2SiO_4 + $CaSi_2O_5$ and $CaSiO_3$ perovskite. The phase boundary between $CaSiO_3$ walstromite and β-Ca_2SiO_4 + $CaSi_2O_5$ is also calculated by using calorimetric enthalpy data.

Experimental methods

Sample syntheses

Wollastonite solid solutions in the $CaSiO_3$–$CaGeO_3$ system were prepared as starting materials for the high-pressure synthesis of perovskites. $CaSiO_3$ wollastonite was synthesized by heating a mixture of reagent grade $CaCO_3$ and silicic acid ($SiO_2 \cdot xH_2O$) at 1353 K for 150 h. The other end member, $CaGeO_3$ wollastonite, was prepared by heating a mixture of reagent grade $CaCO_3$ and GeO_2 at 1373 K for 48 h. $CaSiO_3$ wollastonite was mixed with $CaGeO_3$ to make $Ca(Si_{0.1}Ge_{0.9})O_3$, $Ca(Si_{0.2}Ge_{0.8})O_3$, and $Ca(Si_{0.3}Ge_{0.7})O_3$. These mixtures were pressed into pellets and heated for 250–350 h at 1353 K. This reaction temperature was chosen to prevent $CaSiO_3$ wollastonite from changing to pseudowollastonite (Osborn and Schairer 1941). The pellets were reground and mixed for 1 h in an agate mortar under ethanol. Three to five cycles of heating and grinding were done for each wollastonite solid solution. The $CaSiO_3$ wollastonite sample for drop-solution calorimetry was prepared by heating at 2 Gpa and 1473 K for 1 h using a piston-cylinder high-pressure apparatus (Depths of the Earth Co.). The $CaSiO_3$ wollastonite synthesized at atmospheric pressure was used as a starting material. The recovered sample was confirmed by XRD to be pure single-phase wollastonite.

Perovskite solid solutions in the $CaSiO_3$–$CaGeO_3$ system were synthesized using a multianvil high-pressure apparatus at Gakushuin University (Suzuki and Akaogi 1995). Tungsten carbide anvils with 8-mm truncated edge length (TEL) were used for $CaGeO_3$ perovskite synthesis. Tungsten carbide anvils with 5-mm TEL were used for all other perovskite solid solution syntheses. Powdered starting materials were put in a Pt capsule which also served as a heater. The synthesis temperatures were measured with a Pt/Pt · 13%Rh thermocouple placed at the central part of the sample. $CaGeO_3$ perovskite was synthesized at 9.5 GPa and 1073 K for 1 h. $Ca(Si_{0.1}Ge_{0.9})O_3$, $Ca(Si_{0.2}Ge_{0.8})O_3$ and $Ca(Si_{0.3}Ge_{0.7})O_3$ perovskites were synthesized at 15.5 GPa and 1273 K for 1 h. The quenched samples were examined by powder X-ray diffraction, microfocus X-ray diffraction, and microprobe analysis. The analyses showed that the synthesized perovskites were single-phase and had homogeneous compositions.

Calorimetry

Calorimetric experiments were performed using the ultrasensitive solution calorimeter described in Topor and Navrotsky (1992). This calorimeter is an optimized version of the normal Calvet type microcalorimeter (Navrotsky 1977, 1997). The calorimeter was calibrated by dropping pellets of powdered α-Al_2O_3 (2 mg), the heat capacity of which is well known (e.g., Richet and Fiquet 1991).

In this study, 2–3 mg of the powdered samples were pressed into pellets and dropped into the calorimeter. Enthalpies of drop solution for the perovskite solid solutions in the $CaSiO_3$–$CaGeO_3$ system and $CaSiO_3$ wollastonite were measured by dropping the samples from 298 K into molten $2PbO \cdot B_2O_3$ solvent (1.5 g) at 974 K. As many as three drops on each side for each sample were performed. After each set of experiments, examination of the quenched lead borate glass by optical microscopy confirmed that the samples had completely dissolved in the solvent.

Results and discussion

Unit-cell volumes of the solid solutions

Unit cell volumes of the $CaGeO_3$–$CaSiO_3$ solid solutions obtained by powder X-ray diffraction are shown in Fig. 1 and Table 1. Lattice parameters of all of them were refined by using orthorhombic system. The obtained *a*-axis and *b*-axis parameters for the solid solutions are the same within the errors. However, the observed XRD peak profiles of the perovskite solid solutions are very similar to that of pure $CaGeO_3$ perovskite. Therefore it is thought that phase transition might not happen in the composition range of synthesized samples. The unit-cell volume decreases linearly with increasing $CaSiO_3$ component up to 30 mol%. If the least-squares fitted line of the unit-cell volume data is extrapolated to the $CaSiO_3$ end member, a unit-cell volume for $CaSiO_3$ perovskite of 183.3 ± 1.0 Å^3 (the same unit cell as for an orthorhombic perovskite) is obtained. The unit-cell volume is in agreement with those determined from high-pressure experiments (e.g., 182.3 ± 0.3 Å^3; Yagi et al. 1989; 183.3 ± 0.3 Å^3; Wang and Weidner 1994). Because the space groups for $CaSiO_3$ perovskite (*Pm*3*m*) and $CaGeO_3$ perovskite (*Pbnm*) are different, perovskites in the $CaSiO_3$–$CaGeO_3$ system cannot be a continuous solid solution. However, by considering the small deformation of $CaGeO_3$ perovskite from an ideal perovskite structure, the results suggest that any volume change accompanying the phase transition between *Pbnm* and *Pm*3*m* is negligible and that the perovskite solid solutions in the $CaSiO_3$–$CaGeO_3$ can be regarded as the pseudoideal in terms of volume.

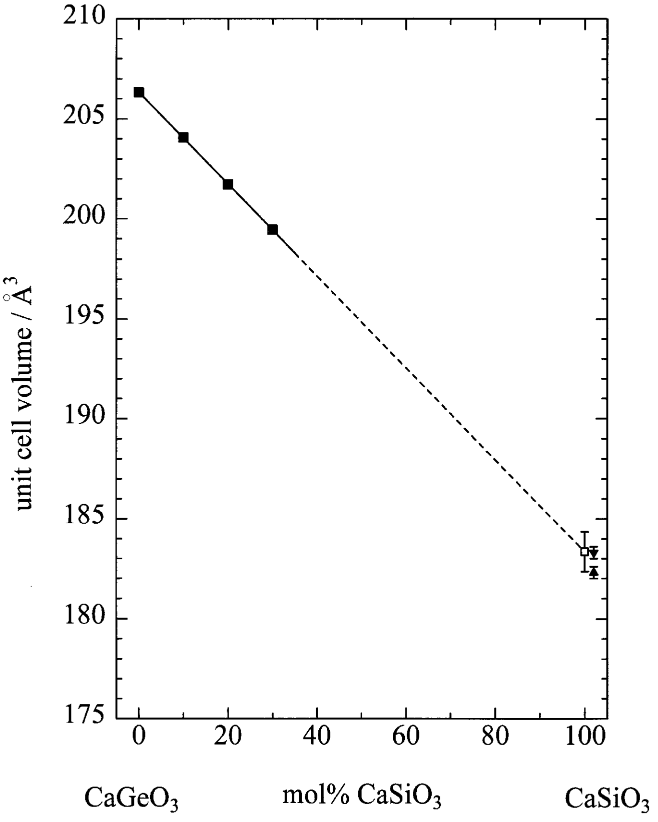

Fig. 1 Unit-cell volumes of perovskite solid solutions in the $CaSiO_3$–$CaGeO_3$ system. *Solid squares* and *open square* show a measured perovskite solid solution unit cell volume and estimated $CaSiO_3$ perovskite unit-cell volume, respectively. The *solid line* and *its dashed extension* are a least-squares fits to *solid square* data. *Solid triangles* indicate the unit-cell volume of $CaSiO_3$ perovskite determined by high-pressure experiment; ▲ (Yagi et al. 1989), ▼ (Wang and Weidner 1994)

Table 1 Lattice parameters and unit-cell volumes of perovskite solid solutions in the $CaSiO_3$–$CaGeO_3$ system

Composition	a/Å	b/Å	c/Å	V/Å^3
$CaGeO_3$	5.262(2)	5.267(3)	7.444(2)	206.3(1)
$Ca(Si_{0.1}Ge_{0.9})O_3$	5.249(3)	5.242(5)	7.417(3)	204.1(1)
$Ca(Si_{0.2}Ge_{0.8})O_3$	5.229(3)	5.220(5)	7.390(3)	201.7(1)
$Ca(Si_{0.3}Ge_{0.7})O_3$	5.207(2)	5.203(3)	7.362(2)	199.4(1)

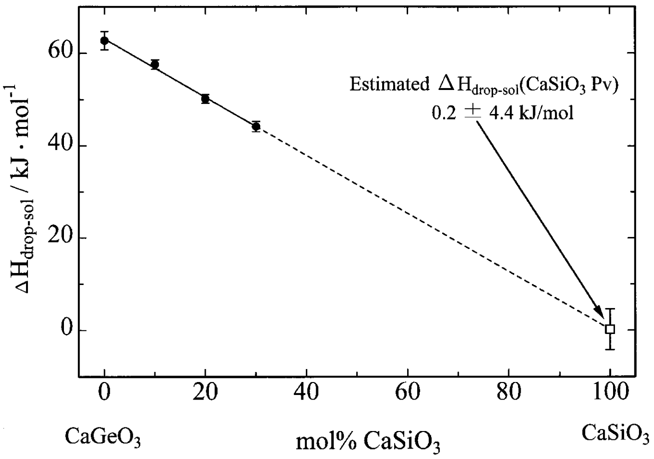

Fig. 2 Drop-solution enthalpy of $CaSiO_3$–$CaGeO_3$ perovskite solid solutions. *Solid circles* show measured drop-solution enthalpy. *Open square* indicates an estimated drop-solution enthalpy for $CaSiO_3$ perovskite. The *solid line* and *its dashed extension* are a least-squares fit to four measured data

Table 2 Drop-solution enthalpies of perovskites and wollastonite

Composition	Sample weight (mg)	$\Delta H_{drop-sol}$ (kJ mol^{-1})
$CaGeO_3$ (pv)	2.410	61.12
	2.934	65.52
	2.598	63.18
	2.566	61.87
	2.928	59.28
	2.578	65.22
	Average 62.70 ± 1.98	
$Ca(Si_{0.1}Ge_{0.9})O_3$ (pv)	2.419	57.41
	2.467	58.89
	2.523	58.11
	2.436	55.81
	2.487	57.60
	Average 57.56 ± 1.02	
$Ca(Si_{0.2}Ge_{0.8})O_3$ (pv)	2.466	50.11
	2.495	48.94
	2.558	50.40
	2.416	49.70
	2.273	51.71
	Average 50.17 ± 0.91	
$Ca(Si_{0.3}Ge_{0.7})O_3$ (pv)	2.368	43.60
	2.431	43.27
	2.428	43.43
	2.487	46.29
	2.475	44.38
	Average 44.20 ± 1.12	
$CaSiO_3$ (wo)	2.470	104.47
	2.251	105.21
	2.330	105.13
	2.380	103.81
	2.288	104.52
	Average 104.63 ± 0.51	

Measured enthalpies

The calorimetric data are shown in Fig. 2 and in Table 2. The drop-solution enthalpy of $CaGeO_3$ perovskite of 62.70 ± 1.98 kJ mol^{-1} is consistent with the previous value of 60.87 ± 4.19 kJ mol^{-1} calculated from the heat content and solution enthalpy data for $CaGeO_3$ wollastonite and the phase transition enthalpy of $CaGeO_3$ (pv → wo) (Ross et al. 1986). The data in Fig. 2 indicate that the drop-solution enthalpy ($\Delta H_{drop-sol}$) of perovskite solid solutions in the $CaSiO_3$–$CaGeO_3$ system decreases linearly with increasing $CaSiO_3$ component. If the phase transition enthalpy between *Pbnm* and *Pm*3*m* phases is assumed to be negligible, as consistent with the unit-cell volume and by considering the small deformation from an ideal cubic perovskite, we can approximate the perovskite solid solution in the $CaSiO_3$–$CaGeO_3$ system as ideal in terms of enthalpy. This assumption allows us to estimate the $\Delta H_{\text{drop-sol}}$ of $CaSiO_3$ perovskite by a linear extrapolation of the data obtained in this study. By extrapolating the least-squares fitted line of the four $\Delta H_{\text{drop-sol}}$ data to the $CaSiO_3$ end member, the $\Delta H_{\text{drop-sol}}$ of $CaSiO_3$ perovskite from 298 to 974 K in $2PbO \cdot B_2O_3$ solvent is calculated as 0.2 ± 4.4 kJ mol^{-1}. In this study, $\Delta H_{\text{drop-sol}}$ of $CaSiO_3$ wollastonite was also measured to be 104.6 ± 0.5 kJ mol^{-1}. This value is within error of that reported by Chai and Navrotsky (1993) of 105.4 ± 0.7 kJ mol^{-1}. The wollastonite–perovskite phase transition enthalpy in $CaSiO_3$ at 298 K [$\Delta H^{\circ}_{\text{tr},298}$ ($CaSiO_3$, wo $\rightarrow$ pv)] of 104.4 ± 4.4 kJ mol^{-1} was calculated from the difference between the $\Delta H_{\text{drop-sol}}$ of $CaSiO_3$ perovskite and that of wollastonite. Koito et al. (2000) also estimated the $\Delta H^{\circ}_{\text{tr},298}$ ($CaSiO_3$, wo $\rightarrow$ pv) by calorimetry of perovskite solid solutions in the $CaTiO_3$–$CaSiO_3$ system. Despite a considerable extrapolation in both studies, the value of Koito et al. (2000) of 109.5 ± 6.3 kJ mol^{-1} is consistent within error with the value obtained in this study.

A relatively well-constrained formation enthalpy ($\Delta H^{\circ}_{\text{f},298}$) from CaO (lime) + SiO_2 (quartz) for $CaSiO_3$ wollastonite (-89.61 ± 0.21 kJ mol^{-1}) was given by Zhu et al. (1994). The $\Delta H^{\circ}_{\text{f},298}$ ($CaSiO_3$ wo) and $\Delta H^{\circ}_{\text{f},298}$ ($CaSiO_3$, wo $\rightarrow$ pv) yield the formation enthalpy of $CaSiO_3$ perovskite $\Delta H^{\circ}_{\text{f},298}$ ($CaSiO_3$ pv) from CaO + SiO_2 quartz of 14.8 ± 4.4 kJ mol^{-1}, or that from CaO + SiO_2 stishovite of -22.2 ± 4.5 kJ mol^{-1}, which is calculated using $\Delta H^{\circ}_{\text{tr},298}$ (SiO_2 qz $\rightarrow$ st) $= 37.01 \pm 0.98$ kJ mol^{-1} (Akaogi et al. 1995). This value is about 20 kJ mol^{-1} more positive than the estimation by Swamy and Dubrovinsky (1997) (-5.1 kJ mol^{-1} from CaO + quartz), which was determined using a quasi-harmonic lattice dynamic method combined with high-pressure experimental results by Gasparik et al. (1994).

Crystal chemistry of perovskite

The stability of $A^{2+}B^{4+}O_3$ perovskite compounds was discussed by Takayama-Muromachi and Navrotsky (1988) using a lattice energy approach. The internal energy of an ionic crystal can be separated into two terms:

$$E = E_M + E_N \ , \tag{1}$$

where E_M is the electrostatic (Madelung) energy and E_N includes all other interaction energies, among which the repulsion energy gives the largest contribution. For the reaction:

$$AO + BO_2 = ABO_3 \text{ (perovskite)} \tag{2}$$

the internal energy difference between the product and the reactant is essentially the same as the formation enthalpy of perovskite from the oxide components (ΔH°_{f}). Therefore, the formation enthalpy from the oxide components can be represented as

$$\Delta H^{\circ}_{f} \fallingdotseq \Delta E = \Delta E_M + \Delta E_N , \tag{3}$$

where ΔE_M and ΔE_N are the electrostatic energy difference and the nonelectrostatic energy difference between the product and the reactant in Eq. (2), respectively.

The variation of ΔE_N with tolerance factor is shown in Fig. 3. The data to calculate ΔE_N are in Table 3. The tolerance factor is given by

$$t = (r_A + r_O)/\sqrt{2}(r_B + r_O) \ , \tag{4}$$

where r_A, r_B, and r_O refer to the ionic radius of A^{2+}, B^{4+} and O^{2-}, respectively (Shannon and Prewitt 1969). Takayama-Muromachi and Navrotsky (1988) used a fixed A^{2+} coordination of 8 for Mg, Cd, and Ca and 12 for Sr, Pb, and Ba. In this study, r_A was chosen by taking into account the crystal structure (8 coordination for orthorhombic and 12 coordination for cubic). As seen in Fig. 3, ΔE_N decreases approximately linearly with increasing tolerance factor. $MgSiO_3$ and especially $CaSiO_3$ perovskites, which are stable at high pressure only, deviate from the trend line. This extra destabilizing energy in $CaSiO_3$ perovskite may be a partial explanation of why the high-pressure $CaSiO_3$ perovskite cannot be quenched to ambient pressure. Computer simulations of the stability of $CaSiO_3$ perovskite show that the lowest F_{1u} transverse optic vibrational mode becomes

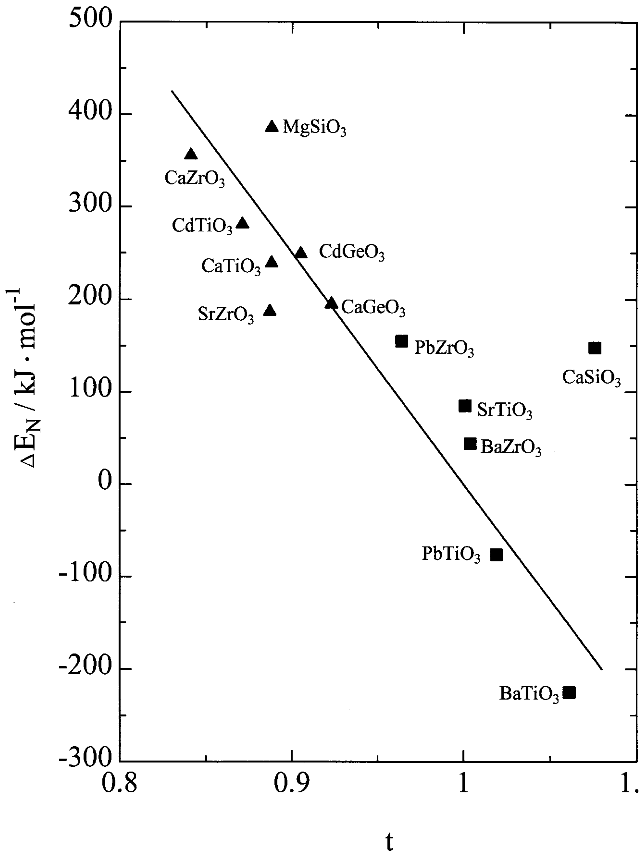

Fig. 3 Relationship between nonelectrostatic energy and tolerance factor. *Triangles* and *squares* show orthorhombic and cubic perovskite data, respectively. *Solid line* is a trend line. See text for further explanation

Table 3 Formation enthalpy from oxides, electrostatic (ΔE_M) and nonelectrostatic (ΔE_N) energy of perovskite formation

Compound	ΔH_f° (kJ mol^{-1})	ΔE_M^a (kJ mol^{-1})	ΔE_N (kJ mol^{-1})
$CaTiO_3$	−80.9 ± 2.3[a]	−319	238
$SrTiO_3$	−135.1 ± 2.2[a]	−221	86
$BaTiO_3$	−152.3 ± 4.0[a]	73	−225
$PbTiO_3$	−31.1 ± 4.1[a]	45	−76
$CdTiO_3$	−22.3 ± 2.4[a]	−304	282
$CaZrO_3$	−31.3 ± 4.0[a]	−387	356
$SrZrO_3$	−75.9 ± 4.5[a]	−263	187
$BaZrO_3$	−123.9 ± 4.1[a]	−168	44
$PbZrO_3$	1.7 ± 6.6[a]	−154	156
$CaGeO_3$	−37.3 ± 2.7[b]	−232	195
$CdGeO_3$	27.5 ± 3.5[c]	−222	250
$MgSiO_3$	28.4 ± 5.3[d]	−358	386
$CaSiO_3$	−22.2 ± 4.5[b]	−170	148

[a] Takayama-Muromachi and Navrotsky (1988). PbO is not a rocksalt but a massicot (yellow) structure. ZrO_2 is a baddeleyite structure. Other divalent oxides are rocksalt, tetravalent are rutile

[b] This study, formation enthalpy at 298 K from rocksalt + rutile structure

[c] Akaogi and Navrotsky (1987), formation enthalpy at 298 K from rocksalt + rutile structure

[d] Akaogi and Ito (1993), formation enthalpy at 298 K from rocksalt + rutile structure

unstable under tension near atmospheric pressure, and that the unstable vibrational mode triggers amorphization of the cubic phase (Hemmati et al. 1995; Chizmeshya et al. 1996). The excess nonelectrostatic energy might be related to the unstable vibrational mode. It seems likely that the excess energy caused by the instability of lattice vibrations decreases the energy barrier between the perovskite phase and the *P*4*mm* phase, an intermediate phase prior to the amorphous phase (Hemmati et al. 1995).

In an orthorhombic perovskite, the size of the A^{2+} site is adjusted by tilting the $B^{4+}O_6$ octahedra. If the geometry of the orthorhombic perovskite structure is considered, it is expected that the repulsion energy is related to the degree of tilting as well as the tolerance factor. Therefore, we took the angle ϕ, which is the rotation angle of the $B^{4+}O_6$ octahedra from that in the ideal perovskite (e.g., O'Keeffe et al. 1979) as a measure of the distortion from cubic symmetry. A plot of ΔE_N against ϕ is shown in Fig. 4. Because the ΔE_N of $MgSiO_3$ perovskite seems to deviate somewhat from the trend in Fig. 3 especially, the relationship between tolerance factor and ΔE_N is not obvious. On the other hand, a good linear relationship (R^2 factor = 0.95) is seen in Fig. 4. This relation in Fig. 4 reflects the fact that a larger degree of tilting results in closer oxygen–oxygen distances among $B^{4+}O_6$ octahedra.

High-pressure phase equilibrium relations in the $CaSiO_3$ system

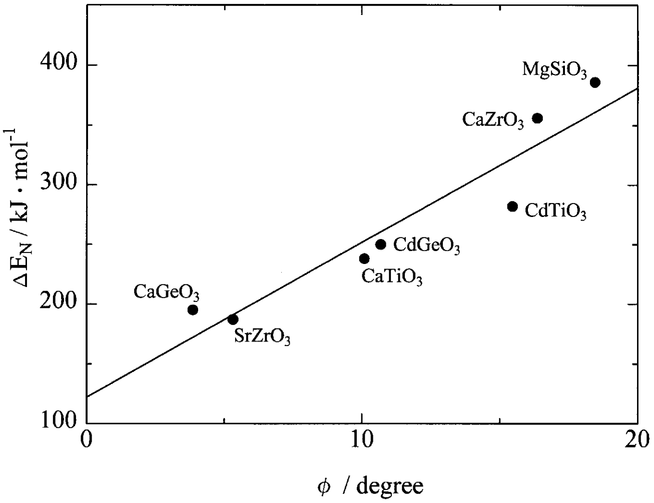

Fig. 4 Relationship between nonelectrostatic energy and rotation angle ϕ of BO_6 octahedra for orthorhombic (distorted) perovskites. *Solid line* shows linear fit of all the data

Using the formation enthalpy for $CaSiO_3$ perovskite obtained in this study, the phase equilibrium boundary between $CaSiO_3$ perovskite and β-Ca_2SiO_4 + $CaSi_2O_5$ was calculated. A calculation of the phase boundary between β-Ca_2SiO_4 + $CaSi_2O_5$ and $CaSiO_3$ walstromite was also made by adopting a calorimetric enthalpy for $CaSi_2O_5$ (Schoenitz et al. 2001).

Thermodynamic parameters for those materials determined experimentally are very limited. Therefore, for the phase boundary calculations, the following simplified thermodynamic equation;

$$\Delta G_{P,T} = \Delta H^\circ - T\Delta S^\circ + P\Delta V^\circ = 0 \quad (5)$$

is used as a first approximation, where ΔH°, ΔS° and ΔV° are enthalpy, entropy, and volume changes at ambient conditions, respectively. ΔS° was determined by using ΔH° and ΔV° and by setting $\Delta G(P,T) = 0$ at one reference (P,T) point assumed to be on the equilibrium phase boundary (hereafter called a fixing point). We chose not to consider the effects of heat capacity, thermal expansion, and compressibility because these values are poorly known, though there have been several attempts to estimate them (e.g., Swamy and Dubrovinsky 1997). Thermodynamic parameters used for the phase boundary calculations are shown in Table 5.

In Fig. 5, high-pressure experimental results by Gasparik et al. (1994) and Wang and Weidner (1994) are plotted. The point at 9.5 GPa and 1423 K by Gasparik et al. (1994) is taken as lying on the phase boundary between $CaSiO_3$ walstromite and β-Ca_2SiO_4 + $CaSi_2O_5$. From this point and our measured ΔH°, we obtained $\Delta S^\circ = -32.7 \pm 4.5$ J K^{-1} for the reaction $3CaSiO_3$ walstromite $\rightarrow$ β-Ca_2SiO_4 + $CaSi_2O_5$ (three moles $CaSiO_3$ basis). This uncertainty in ΔS° is propagated from the uncertainty of the enthalpy change for the reaction. Additional uncertainties arise both from the assumption of constant ΔH, ΔS, and ΔV of reactions and from uncertainties in P and T for the point on the phase boundary. Their magnitude is difficult to quantify,

Table 4 Nonelectrostatic energy and degree of tilting of octahedra for orthorhombic perovskites. $\phi = \cos^{-1}(\sqrt{2}a^2/bc)$: the rotation angle of octahedra in degree

Compound	ΔE_N (kJ mol^{-1})	Lattice parameters			ϕ
		a/Å	b/Å	c/Å	
$CaTiO_3$	238	5.3796(1)	5.4423(3)	7.6401(5)[a]	10.103
$CdTiO_3$	282	5.3053(1)	5.4215(3)	7.6176(3)[a]	15.459
$CaZrO_3$	356	5.5929(6)	5.7558(3)	8.0101(14)[b]	16.362
$SrZrO_3$	187	5.797(1)	5.8179(5)	8.204(2)[c]	5.314
$CaGeO_3$	195	5.2607(6)	5.2688(10)	7.4452(15)[d]	3.859
$CdGeO_3$	250	5.209(1)	5.253(1)	7.434(1)[e]	10.692
$MgSiO_3$	386	4.7754(3)	4.9292(4)	6.8969(5)[f]	18.442

[a] Sasaki et al. (1987)
[b] JCPDS 35–790 (1985)
[c] JCPDS 44–161 (1994)
[d] Sasaki et al. (1983)
[e] Susaki (1989)
[f] Ito and Matsui (1978)

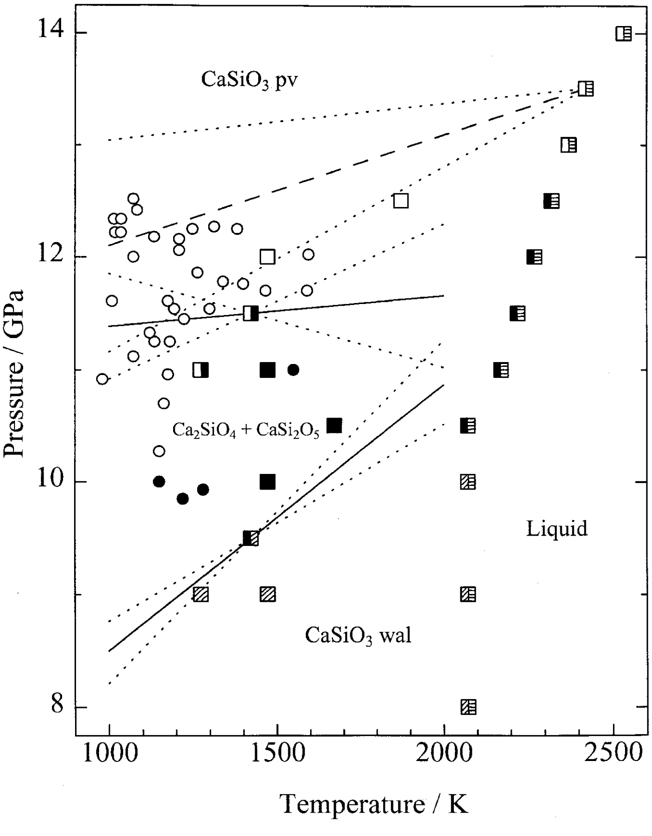

Fig. 5 Phase relations in the $CaSiO_3$ system. *Squares* and *circles* are high-pressure experimental results by Gasparik et al. (1994) and by Wang and Weidner (1994), respectively. *Open*, *closed*, *hatched*, and *horizontal striped symbols* show $CaSiO_3$ perovskite, β-Ca_2SiO_4 + $CaSi_2O_5$, $CaSiO_3$ walstromite, and liquid phases, respectively. *Solid* and *dashed lines* are phase boundaries calculated from thermodynamic data. The *lower solid line* is phase boundary between β-Ca_2SiO_4 + $CaSi_2O_5$ and $CaSiO_3$ walstromite, the *upper solid line* and *dashed line* represent the phase boundary between $CaSiO_3$ perovskite and β-Ca_2SiO_4 + $CaSi_2O_5$ by using the data point at 11.5 GPa and 1423 K and the triple point at 13.5 GPa and 2423 K by Gasparik et al. (1994) as a fixing point, respectively. *Dotted lines* represent errors of the calculated phase boundaries. See text for further discussion

Table 5 Thermodynamic parameters used for phase boundary calculations; *wal* walstromite; *pv* perovskite

Phase	$\Delta H^\circ_{f,298}$ (kJ mol^{-1})	V°_{298} (cm^3 mol^{-1})
$CaSiO_3$ wal	−78.90 ± 1.42[a]	37.94[e]
β-Ca_2SiO_4	−125.80 ± 2.09[b]	51.78[f]
$CaSi_2O_5$	−26.32 ± 4.27[c]	48.24[g]
$CaSiO_3$ pv	14.79 ± 4.41[d]	27.45[h]

[a] Charlu et al. (1978), corrected with Cp for CaO and SiO_2 (quartz) by Robie and Hemingway (1995) and Cp for $CaSiO_3$ walstromite (wollastonite II tc) by Halbach and Chatterjee (1984)
[b] Haas et al. (1981), corrected to formation enthalpy from oxide using formation enthalpies for CaO and SiO_2 (quartz) by Robie and Hemingway (1995)
[c] Schoenitz et al. (2001)
[d] This study
[e] Chatterjee et al. (1984)
[f] Jost et al. (1977)
[g] Kanzaki et al. (1991)
[h] Wang et al. (1996)

but a doubling of the error in ΔS° is not unreasonable, giving $\Delta S^\circ = -32.7 \pm 9.0$ J K^{-1} when all sources of error are considered. The phase boundary is calculated as $P = 2.4 \times 10^{-3} \pm 6.5 \times 10^{-4}\ T + 6.1 \pm 0.7$, where P and T are in GPa and in K, respectively. Although the calculated slope is slightly steeper than that given by Gasparik et al. (1994) (1.4×10^{-3} GPa K^{-1}), it is still consistent with the high-pressure experimental result within the error.

The phase boundary between β-Ca_2SiO_4 + $CaSi_2O_5$ and $CaSiO_3$ perovskite was calculated in a similar way. Gasparik et al. (1994) observed coexistence of $CaSiO_3$ perovskite with β-Ca_2SiO_4 + $CaSi_2O_5$ near 11.5 GPa in the temperature range 1300–1500 K. Therefore, we first chose the data point at 11.5 GPa, 1423 K by Gasparik et al. (1994) as a fixing point for the phase boundary calculation. The phase boundary is calculated as $P = 2.7 \times 10^{-4} \pm 1.1 \times 10^{-3}\ T + 11.1 \pm 1.0$ (GPa). The calculated boundary has a somewhat less steep slope than that given by Gasparik et al. (1994) (2.1×10^{-3} GPa K^{-1}), and is not consistent with high-pressure experimental data above about 2000 K.

Table 6 Thermochemical data for high-pressure and high-temperature phase relations in the $CaSiO_3$ system. ΔH°_{298} and ΔV°_{298} are values on the basis of 3 mol $CaSiO_3$

Reaction	ΔH°_{298} (kJ)	ΔV°_{298} (cm^3)	P (GPa)	T (K)	ΔS° ($J\ K^{-1}$)	dP/dT ($GPa\ K^{-1}$)
$3CaSiO_3$ wal $\rightarrow Ca_2SiO_4 + CaSi_2O_5$	84.58 ± 6.38	−13.80	9.5	1423	−32.7	2.4×10^{-3}
$Ca_2SiO_4 + CaSi_2O_5 \rightarrow 3CaSiO_3$ pv	196.49 ± 14.06	−17.67	11.5	1423	−4.7	2.7×10^{-4}
			13.5	2423	−17.4	9.8×10^{-4}

Gasparik et al. (1994) used $CaSiO_3$ wollastonite as the starting material. Because the P–T path of the experiment for the fixing point goes through the $CaSiO_3$ perovskite phase field during heating, a phase transition from $CaSiO_3$ wollastonite to $CaSiO_3$ perovskite might take place first. When the temperature gradient of 200 K in their sample capsule is considered, it is possible that $CaSiO_3$ perovskite coexisting with β-Ca_2SiO_4 + $CaSi_2O_5$ at 11.5 GPa and 1423 K and also at 11.0 GPa and 1273 K is metastable due to slow diffusion rates in the lower temperature region of the sample capsule. Therefore, it is suggested that the phase equilibrium boundary might be at higher pressure than the boundary calculated using this fixing point.

Since a faster and more complete reaction is expected at higher temperature, we chose next the reported triple point at 13.5 GPa and 2423 K among $CaSiO_3$ perovskite, β-Ca_2SiO_4 + $CaSi_2O_5$, and $CaSiO_3$ liquid by Gasparik et al. (1994) as a fixing point. From this fixing point, ΔS° is calculated to be $-17.4 \pm 11.6\ J\ K^{-1}$. Then a phase boundary is obtained as $P = 9.8 \times 10^{-4} \pm 6.6 \times 10^{-4}\ T + 11.1 \pm 1.3$ (GPa). This phase boundary appears inconsistent with experimental data at lower temperature. However, the position of the triple point contains considerable uncertainty because the experiments were performed at more than 2300 K. Particularly, Gasparik et al. (1994) applied a pressure calibration obtained under high temperature only up to 1873 K. If the temperature effect on the pressure calibration curve is taken into account, the triple point might be placed at lower pressure. Hence we suggest that a plausible phase equilibrium boundary for the reaction β-Ca_2SiO_4 + $CaSi_2O_5 \rightarrow 3CaSiO_3$ perovskite might be positioned between the two phase boundaries calculated above. In comparing the calculated result with the experimental data by Wang and Weidner (1994), $CaSiO_3$ perovskite exists at lower pressure than the calculations suggest at temperatures below 1200 K. This gives the experimental phase boundary an apparently much steeper slope. Judging from the P–T path of their experiments, these $CaSiO_3$ perovskites could be explained as metastable due to slow dissociation of $CaSiO_3$ perovskite to β-Ca_2SiO_4 + $CaSi_2O_5$. We suggest that dissociation reactions involving nucleation and long-range diffusion may have difficulty reaching equilibrium below 1500 K for short run duration. This hypothesis is consistent with difficulties encountered in attaining equilibrium in the coesite–stishovite reaction below about 1300 K (Zhang et al. 1996). We therefore conclude that the thermochemical data and various attempts to obtain P–T boundaries in the $CaSiO_3$ system can probably be reconciled, but that, at present, the phase diagram, especially for the perovskite boundary, remains poorly constrained. True reversals of at least one point on each boundary, under conditions where P and T are well controlled and calibrated, would be a valuable next step.

Acknowledgements This research was supported by the Center for High Pressure Research (CHiPR), an NSF Science and Technology Center.

References

Akaogi M, Navrotsky A (1987) Calorimetric study of high-pressure phase transitions among the $CdGeO_3$ polymorphs (pyroxenoid, garnet, ilmenite, and perovskite structures). Phys Chem Miner 14: 435–440

Akaogi M, Ito E (1993) Refinement of enthalpy measurement of $MgSiO_3$ perovskite and negative pressure-temperature slopes for perovskite-forming reactions. Geophys Res Lett 20: 1839–1842

Akaogi M, Yusa H, Shiraishi K, Suzuki T (1995) Thermodynamic properties of α-quartz, coesite, and stishovite and equilibrium phase relations at high pressures and high temperatures. J Geophys Res 100: 22337–22347

Chai L, Navrotsky A (1993) Thermochemistry of carbonate-pyroxene equilibria. Contrib Mineral Petrol 114: 139–147

Charlu TV, Newton RC, Kleppa OJ (1978) Enthalpy of formation of some lime silicates by high-temperature solution calorimetry, with discussion of high-pressure phase equilibria. Geochim Cosmochim Acta 42: 367–375

Chatterjee ND, Johannes W, Leistner H (1984) The system CaO–Al_2O_3–SiO_2–H_2O: new phase equilibria data, some calculated phase relations, and their petrological applications. Contrib Mineral Petrol 88: 1–13

Chizmeshya AVG, Wolf GH, McMillan PF (1996) First-principles calculation of the equation-of-state, stability, and polar optic modes of $CaSiO_3$ perovskite. Geophys Res Lett 23: 2725–2728

Gasparik T, Wolf K, Smith CM (1994) Experimental determination of phase relations in the $CaSiO_3$ system from 8 to 15 GPa. Am Mineral 79: 1219–1222

Haas JL Jr, Robinson GR Jr, Hemingway BS (1981) Thermodynamic tabulations for selected phases in the system CaO–Al_2O_3–SiO_2–H_2O at 101.325 kPa (1 atm) between 273.15 and 1800 K. J Phys Chem Ref Data 10: 575–669

Halbach H, Chatterjee ND (1984) An internally consistent set of thermodynamic data for 21 CaO–Al_2O_3–SiO_2–H_2O phases by linear parametric programming. Contrib Mineral Petrol 88: 14–23

Hemmati M, Chizmeshya A, Wolf GH, Poole PH, Shao J, Angell CA (1995) Crystalline-amorphous transition in silicate perovskites. Phys Rev (B) 51: 14841–14848

Irifune T, Ringwood AE (1987) Phase transformations in primitive MORB and pyrolite compositions to 25 GPa and some geophysical implications. In: Manghnani MH, Syono Y (eds) High-pressure research in mineral physics. Terra Scientific Publishing Co., Tokyo/Am Geophys Union, Washington, DC, pp 231–242

Ito E, Matsui Y (1978) Synthesis and crystal-chemical characterization of $MgSiO_3$ perovskite. Earth Planet Sci Lett 38: 443–450

Joint committee on powder diffraction standards, no. 35-790 (1985)

Joint committee on powder diffraction standards, no. 44-161 (1994)

Jost KH, Ziemer B, Seydel R (1977) Redetermination of the structure of β-dicalcium silicate. Acta Crystallogr (B)33: 1696–1700

Kanzaki M, Stebbins JF, Xue X (1991) Characterization of quenched high-pressure phases in $CaSiO_3$ system by XRD and ^{29}Si NMR. Geophys Res Lett 18: 463–466

Koito S, Akaogi M, Kubota O, Suzuki T (2000) Calorimetric measurements of perovskites in the system $CaTiO_3$–$CaSiO_3$ and experimental and calculated phase equilibria for high-pressure dissociation of diopside. Phys Earth Planet Inter 120: 1–10

Leinenweber K, Grzechnik A, Voorhees M, Navrotsky A, Yao A, McMillan PF (1997) Structural variation in $Ca(Ti_xSi_{1-x})O_3$ perovskites ($1 > x > 0.65$) and the ordered phase Ca_2TiSiO_6. Phys Chem Miner 24: 528–534

Liu L, Ringwood AE (1975) Synthesis of a perovskite-type polymorph of $CaSiO_3$. Earth Planet Sci Lett 28: 209–211

Navrotsky A (1977) Recent progress and new directions in high-temperature calorimetry. Phys Chem Miner 2: 89–104

Navrotsky A (1997) Progress and new directions in high-temperature calorimetry revisited. Phys Chem Miner 24: 222–241

O'Keeffe M, Hyde BG, Bovin J (1979) Contribution to the crystal chemistry of orthorhombic perovskites: $MgSiO_3$ and $NaMgF_3$. Phys Chem Miner 4: 209–305

Osborn EF, Schairer JF (1941) The ternary system pseudowollastonite–akermanite–gehlenite. Am J Sci 239: 715–763

Richet P, Fiquet G (1991) High-temperature heat capacity and premelting of minerals in the system MgO–CaO–Al_2O_3–SiO_2. J Geophys Res 96: 445–456

Ringwood AE, Major A (1967) Some high-pressure transformations of geophysical significance. Earth Planet Sci Lett 2: 106–110

Robie R, Hemingway BS (1995) Thermodynamic properties of minerals and related substances at 298.15 K and 1 bar (10^5 Pascals) pressure and at higher temperatures. US Geol Surv Bull 2131

Ross NL, Akaogi M, Navrotsky A, Susaki J, McMillan PF (1986) Phase transitions among the $CaGeO_3$ polymorphs (wollastonite, garnet, and perovskite structures): studies by high-pressure synthesis, high-temperature calorimetry, and vibrational spectroscopy and calculation. J Geophys Res 91: 4685–4696

Sasaki S, Prewitt CT, Liebermann RC (1983) The crystal structure of $CaGeO_3$ perovskite and the crystal chemistry of the $GdFeO_3$-type perovskites. Am Mineral 68: 1189–1198

Sasaki S, Prewitt CT, Bass JD, Schulze WA (1987) Orthorhombic perovskite $CaTiO_3$ and $CdTiO_3$: structure and space group. Acta Crystallogr (C)43: 1668–1674

Schoenitz M, Navrotsky A, Ross NL (2001) Enthalpy of formation of $CaSi_2O_5$, a quenched high-pressure phase with pentacoordinate silicon. Phys Chem Miner 28: 57–60

Shannon RD, Prewitt CT (1969) Effective ionic radii in oxides and fluorides. Acta Crystallogr (B)25: 925–946

Susaki J (1989) $CdGeO_3$-phase transformations at high pressure and temperature and structural refinement of the perovskite polymorph. Phys Chem Miner 16: 634–641

Suzuki T, Akaogi M (1995) Element partitioning between olivine and silicate melt under high pressure. Phys Chem Miner 22: 411–418

Swamy V, Dubrovinsky LS (1997) Thermodynamic data for the phases in the $CaSiO_3$ system. Geochim Cosmochim Acta 61: 1181–1191

Takayama-Muromachi E, Navrotsky A (1988) Energetics of compounds ($A^{2+}B^{4+}O_3$) with the perovskite structure. J Solid State Chem 72: 244–256

Topor L, Navrotsky A (1992) Advances in calorimetric techniques for high-pressure phases. In: Syono Y, Manghnani MH (ed) High-pressure research: application to Earth and planetary sciences. Terra Scientific Publishing Co, Tokyo/Am Geophys Union, Washington, DC, pp 71–76

Wang Y, Weidner DJ (1994) Thermoelasticity of $CaSiO_3$ and implications for the lower mantle. Geophys Res Lett 21: 895–898

Wang Y, Weidner DJ, Guyot F (1996), Thermal equation of state of $CaSiO_3$ perovskite. J Geophys Res 101: 661–672

Yagi T, Kusanagi S, Tsuchida U, Fukai Y (1989) Isothermal compression and stability of perovskite-type $CaSiO_3$. Proc Jpn Acad 65: 129–132

Zhang J, Li B, Utsumi W, Liebermann RC (1996) In situ X-ray observations of the coesite-stishovite transition: reversed phase boundary and kinetics. Phys Chem Miner 23: 1–10

Zhu H, Newton RC, Kleppa OJ (1994) Enthalpy of formation of wollastonite ($CaSiO_3$) and anorthite ($CaAl_2Si_2O_8$) by experimental phase equilibrium measurements and high-temperature solution calorimetry. Am Mineral 79: 134–144